The Evanescent Plane Wave Solutions of the Maxwell Equations Revisited. Snell Law and Fresnel Coefficients

Jean-Pierre Bérenger

School of Electrical and Electronic Engineering

The University of Manchester, UK

(Email: jpberenger@gmail.com)

Abstract – **In textbooks on electromagnetism, the plane wave solutions of the Maxwell equations in free space are in most cases limited to homogeneous waves where the field is uniform in any plane perpendicular to the propagation of the phase. However, non homogeneous plane waves where the field is evanescent in a direction perpendicular to the propagation also satisfy the Maxwell equations. This paper revisits such waves that significantly differ from the homogeneous waves. In particular the electromagnetic field is not transverse, it has a component in the direction of propagation of the phase. The equivalents of the Snell law and of the Fresnel coefficients are derived for the reflection and transmission of evanescent plane waves at interfaces, and it is shown that such waves can be generated in the computational domain of numerical methods that solve the Maxwell equations.**

Index Terms—**Electromagnetic theory, Electromagnetic fields, Electromagnetic propagation, Inhomogeneous waves, Evanescent waves, Plane waves, Maxwell equations.**

I. INTRODUCTION

The homogeneous plane wave solutions of the Maxwell equations in a vacuum or in other infinite media, also called traveling waves, play a fundamental role in electromagnetism. The simplicity of the solutions permits theoretical derivations to be performed, concerning the propagation, the reflection, and the refraction of the electromagnetic energy. The plane wave concept is thus essential both for the understanding of most electromagnetic phenomena and in engineering sciences relying on electromagnetism.

Beside the traveling waves, non homogeneous plane waves are also solutions of the Maxwell equations in free space. Such waves widely differ from traveling waves. The electromagnetic field is not transverse, it possesses a component parallel to the direction of propagation of the phase, and it is not uniform in the planes perpendicular to the direction of propagation, where it varies exponentially.

The non homogeneous plane waves, also called evanescent plane waves, are rarely addressed in textbooks on electromagnetism, even at research level. Especially, the existence of these waves is not mentioned in [1, 2, 3, 4]. The only textbook we have found on this question is the one of G.S. Smith [5], where a chapter is devoted to non homogeneous waves. Concerning the literature, we have not found any paper describing with details such waves. We published a paper in 1999 [6] where evanescent plane wave solutions are derived in a vacuum and in the Perfectly Matched Layer (PML) medium. However, [6] is limited to the special two-dimensional (2D) case that allows the reflection observed from the PML absorbing boundary condition to be interpreted.

In the present paper, we revisit the evanescent plane waves in the general three-dimensional case and we derive the corresponding Snell Law and Fresnel reflection and transmission coefficients at interfaces between dielectric media. We also show that evanescent waves can be generated in the computational domain of numerical methods, which is of interest to assess theoretical derivations and to perform experiments involving evanescent fields.

More specifically, in section II the evanescent plane wave solutions of the Maxwell equations are derived in a manner which is different, and we think simpler, than that in [5]. The waves are described with details, in particular the two possible modes where either the electric field or the magnetic field has a component parallel to the propagation of the phase. Explicit expressions of the wavenumbers and of the field components are provided in Cartesian coordinates, which allows such problems as the transmission and reflection of evanescent waves at interfaces to be easily addressed.

In section III the Poynting vector and the relationships that connect the E, H, and k vectors of the waves are derived. Section IV is devoted to numerical experiments with the finite-difference time-domain (FDTD) method [7]. It is demonstrated that evanescent plane waves can be enforced in the FDTD grid where they propagate in accordance with theory. In section V, it is shown that the evanescent fields in some problems, in particular in waveguides and on corrugated surfaces, can be interpreted as a set of evanescent plane waves.

Finally, sections VI and VII address the question of the reflection and transmission of evanescent plane waves at the interface between dielectric media. We have not found any textbook or paper on this question, except for the special case where an evanescent wave is present behind the interface when the incident traveling wave is reflected in totality. Here, the Snell law and the Fresnel coefficients are derived in the general case where the incident plane wave is evanescent. The reflected and transmitted fields are discussed with details, in particular in

some special cases. The theoretical Snell law and Fresnel coefficients are verified by means of numerical experiments with the FDTD method in the case where the evanescence is lying in the plane of incidence.

II. Evanescent Plane Wave Solutions of the Maxwell Equations in Free Space

In this section the waveform and the structure of the field of the plane wave solutions of the Maxwell equations are derived and discussed.

A - The wavenumbers and the waveform

Let us consider harmonic plane waves with the electromagnetic field assumed in the form

$$\psi(\vec{r},t) = \psi_0 e^{j\omega t - j\vec{k}.\vec{r}} \tag{2-1}$$

where ψ is either the E vector, the H vector, or any component of E or H, and where ω is the angular frequency, $\vec{k}$ is the wave vector, and $\vec{r}$ is the position vector. In coordinates (x, y, z) the waveform reads

$$\psi(x,y,z,t) = \psi_0 e^{j\omega t - jk_x x - jk_y y - jk_z z} \tag{2-2}$$

where k_x, k_y, k_z may be real or complex components of the wave vector. By enforcing (2-2) into the Maxwell equations, the equation of dispersion is obtained as:

$$k_x^2 + k_y^2 + k_z^2 = \frac{\omega^2}{c^2} \tag{2-3}$$

where c is the speed of light. For waveform (2-1)-(2-2) to be a solution of the Maxwell equations, wavenumbers k_x, k_y, k_z must satisfy (2-3).

Equations similar to (2-2) and (2-3) also hold in any other coordinates, in particular in coordinates (X, U, V) in Fig. 2-1 with X axis in direction (θ, φ)

$$\psi(X,U,V,t) = \psi_0 e^{j\omega t - jk_X X - jk_U U - jk_V V} \tag{2-4}$$

$$k_X^2 + k_U^2 + k_V^2 = \frac{\omega^2}{c^2} \tag{2-5}$$

where k_X, k_U, k_V are connected to k_x, k_y, k_z by the change of coordinates from (x, y, z) to (X, U, V).

Let us search solutions (k_X, k_U, k_V) that satisfy (2-5). This will provide us with plane wave solutions (2.4) of the Maxwell Equations. A trivial solution to (2-5) is

$$k_X = \pm\frac{\omega}{c}\ ; \quad k_U = 0\ ; \quad k_V = 0 \tag{2-6}$$

Choosing the positive sign of k_x yields the waveform

$$\psi(X,U,V,t) = \psi_0 e^{j\omega t - j\frac{\omega}{c}X} \tag{2-7}$$

This is a traveling plane wave whose phase propagates in direction X (-X if the negative sign of k_X were chosen) and magnitude is uniform in planes perpendicular to X. Using (2-7) into the Maxwell equations expressed in (X, U, V) coordinates, it is easily shown that the components of E and H fields are perpendicular to the direction of propagation X and are perpendicular to each other.

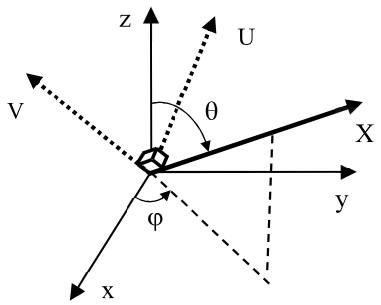

Fig. 2-1. The system of coordinates (X, U, V) with X in direction (θ, φ).

Let us consider again the equation of dispersion (2-5). Solution (2-6)-(2-7) is not the sole solution. It is trivial to verify that the following solution also satisfies (2-5)

$$k_X = \pm\frac{\omega}{c}\cosh\chi \tag{2-8a}$$

$$k_U = \pm j\frac{\omega}{c}\sinh\chi\ \cos\eta \tag{2-8b}$$

$$k_V = \pm j\frac{\omega}{c}\sinh\chi\ \sin\eta \tag{2-8c}$$

where χ and η are two arbitrary real numbers, and where the arbitrary signs of k_U and k_V should be identical and are independent of the sign of k_X. Choosing the positive sign for k_X and the negative sign for k_U and k_V, and inserting these wavenumbers into (2-4), the following waveform is obtained

$$\psi(X,U,V) = \psi_0 e^{-j\frac{\omega}{c}\cosh\chi X}\ e^{-\frac{\omega}{c}\sinh\chi(\cos\eta U + \sin\eta V)} \tag{2-9}$$

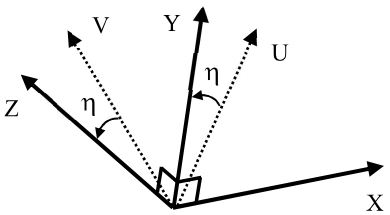

Fig. 2-2. The systems of coordinates (X, U, V) and (X, Y, Z).

Defining now direction Y lying in the (U, V) plane and forming the angle η with U axis (Fig. 2-2), we have $\cos\eta\ U + \sin\eta\ V = Y$, so that (2-9) becomes

$$\psi(X,Y,Z) = \psi_0 e^{-j\frac{\omega}{c}\cosh\chi X}\ e^{-\frac{\omega}{c}\sinh\chi\ Y} \tag{2-10}$$

The wavenumbers (2-8) can then be rewritten in the (X, Y, Z) Cartesian coordinates as

$$k_X = \frac{\omega}{c}\cosh\chi\ ; \quad k_Y = -j\frac{\omega}{c}\sinh\chi\ ; \quad k_Z = 0 \tag{2-11}$$

The plane wave solution of the Maxwell equations in free space (2-10) is thus a wave whose phase propagates in direction X with celerity $c/\cosh\chi$, and whose magnitude is constant in direction Z and evanescent in direction Y, where X, Y, Z are orthogonal. Obviously, by means of other choices of the arbitrary signs in (2-8), the signs in (2-10)-(2-11) could be changed and then the wave could propagate in direction $-X$ or

be evanescent in direction $-Y$. We can notice that changing the sign of χ is equivalent to changing the signs of (2-8b) and (2-8c). In this paper we assume that the signs are those in (2-10)-(2-11), with χ defined as positive or negative which permits the direction of evanescence to be either $+Y$ or $-Y$ for a direction of propagation assumed in $+X$ direction.

For a specified direction of propagation X, the angle η in (2-8) is arbitrary so that the direction of evanescence Y can be any direction perpendicular to X. The evanescence is characterized by the parameter χ. For $\chi = 0$ the magnitude is uniform, the wave is a pure traveling wave, i.e. (2-11) reduces to (2-6). For $\chi \neq 0$, the larger the modulus of χ the stronger the evanescence.

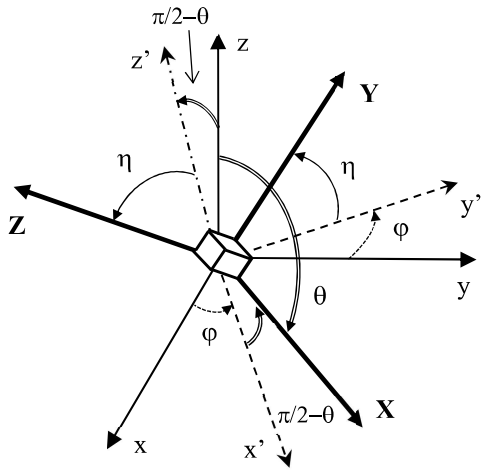

Fig. 2-3. The directions X of propagation of the phase, Y of evanescence, and Z. Starting from axes (x, y, z) a rotation by φ around z gives axes (x', y', z), from which a rotation by $\pi/2 - \theta$ around y' gives axes (X, y', z'), and finally a rotation by η around X gives orthogonal axes (X, Y, Z).

Waveform (2-10) and wavenumbers (2-11) express the evanescent wave in its own system of orthogonal coordinates, where X and Y are the directions of propagation and evanescence, respectively. Obviously, it is possible to express a given physical evanescent wave in any other system. For instance in the system (x, y, z) represented in Fig. 2-3, where propagation X is in direction (θ, φ), and evanescence in direction Y defined with the angle η. By applying the change of coordinates from (X, Y, Z) to (x, y, z) to the wave vector, that is to wavenumbers (2-11), wavenumbers k_x, k_y, k_z are obtained as:

$$k_x = \frac{\omega}{c}\left[\cosh\chi\cos\varphi\sin\theta + j\sinh\chi\left(\cos\varphi\cos\theta\sin\eta + \sin\varphi\cos\eta\right)\right] \quad (2\text{-}12a)$$

$$k_y = \frac{\omega}{c}\left[\cosh\chi\sin\varphi\sin\theta + j\sinh\chi\left(\sin\varphi\cos\theta\sin\eta - \cos\varphi\cos\eta\right)\right] \quad (2\text{-}12b)$$

$$k_z = \frac{\omega}{c}\left[\cosh\chi\cos\theta - j\sinh\chi\sin\theta\sin\eta\right] \quad (2\text{-}12c)$$

It can be verified that the set (2-12) satisfies the equation of dispersion (2-3). And for $\chi = 0$ it reduces to the wavenumbers ($\omega\cos\varphi\sin\theta/c$, $\omega\sin\varphi\sin\theta/c$, $\omega\cos\theta/c$) of a pure traveling wave propagating in direction (θ, φ).

B - The field components of evanescent plane waves

With uniform plane waves, E and H are perpendicular to each other and perpendicular to the direction of propagation. This is no longer true with evanescent waves. To show this, let us consider the Maxwell equations expressed in the (X, Y, Z) coordinates. And let us enforce the six components of the field in the form (2-10) multiplied with $\exp(j\omega t)$, with component magnitudes E_{X0}, E_{Y0}, E_{Z0}, H_{X0}, H_{Y0}, H_{Z0}. The following six equations are obtained

$$\varepsilon_0 c E_{X0} = j\sinh\chi\ H_{Z0} \quad (2\text{-}13a)$$

$$\varepsilon_0 c E_{Y0} = \cosh\chi\ H_{Z0} \quad (2\text{-}13b)$$

$$\varepsilon_0 c E_{Z0} = -\cosh\chi\ H_{Y0} - j\sinh\chi\ H_{X0} \quad (2\text{-}13c)$$

$$\mu_0 c H_{X0} = -j\sinh\chi\ E_{Z0} \quad (2\text{-}13d)$$

$$\mu_0 c H_{Y0} = -\cosh\chi\ E_{Z0} \quad (2\text{-}13e)$$

$$\mu_0 c H_{Z0} = \cosh\chi\ E_{Y0} + j\sinh\chi\ E_{X0} \quad (2\text{-}13f)$$

We can note that (2-13) is composed with two independent subsets, (2-13a)-(2-13b)-(2-13f) and (2-13c)-(2-13d)-(2-13e), respectively. This means that two independent solutions can propagate in direction X and be evanescent in direction Y. Subset (2-13a)-(2-13b)-(2-13f) yields

$$E_{X0} = jZ_0\sinh\chi\ H_0 \quad (2\text{-}14a)$$

$$E_{Y0} = Z_0\cosh\chi\ H_0 \quad (2\text{-}14b)$$

$$H_{z0} = H_0 \quad (2\text{-}14c)$$

and subset (2-13c)-(2-13d)-(2-13e)

$$E_{Z0} = E_0 \quad (2\text{-}15a)$$

$$H_{X0} = -j\frac{1}{Z_0}\sinh\chi\,E_0 \quad (2\text{-}15b)$$

$$H_{Y0} = -\frac{1}{Z_0}\cosh\chi\,E_0 \quad (2\text{-}15c)$$

where H_0 and E_0 are arbitrary constants and Z_0 is the impedance of free space. We denote the two solutions as TM mode and TE mode, with respect to the direction of propagation, respectively.

The TM mode (2-14) has E_Y and H_Z components perpendicular to the direction of propagation, as uniform plane waves. But the ratio of the components is different, $Z_0\cosh\chi$ in place of Z_0. There is an additional E_X component in the direction of propagation. Due to the presence of $j = \exp(j\pi/2)$ in (2-14a), E_X is in advance by $\pi/2$ with respect to E_Y. It vanishes for $\chi = 0$ and equals E_Y in magnitude when χ is large. The physical components corresponding to (2-14) are the real parts of the product of (2-14) with $\exp(-j\omega\cosh\chi\ X/c)$, $\exp(-\omega\sinh\chi\ Y/c)$, and $\exp(j\omega t)$. This yields

$$E_X(X,Y,t) = -Z_0 H_0\sinh\chi\ A_Y\sin(\omega t - \phi_X) \quad (2\text{-}16a)$$

$$E_Y(X,Y,t) = Z_0 H_0\cosh\chi\ A_Y\cos(\omega t - \phi_X) \quad (2\text{-}16b)$$

$$H_z(X,Y,t) = H_0\ A_Y\cos(\omega t - \phi_X) \quad (2\text{-}16c)$$

where

$$A_Y = e^{-\omega\sinh\chi\,Y/c}\ ;\quad \phi_X = \frac{\omega}{c}\cosh\chi\ X \quad (2\text{-}16d)$$

In the TE mode (2-15), the E field is perpendicular to the propagation and the evanescence. There is a H_Y component in the direction of evanescence, and a H_X component in the direction of propagation, in advance by $\pi/2$ with respect to H_Y. This longitudinal H_X vanishes when $\chi = 0$. The physical components corresponding to (2-15) read

$$E_Z(X,Y,t) = E_0\, A_Y \cos(\omega t - \phi_X) \tag{2-17a}$$

$$H_X(X,Y,t) = E_0 / Z_0 \sinh\chi\, A_Y \sin(\omega t - \phi_X) \tag{2-17b}$$

$$H_Y(X,Y,t) = -E_0 / Z_0 \cosh\chi\, A_Y \cos(\omega t - \phi_X) \tag{2-17c}$$

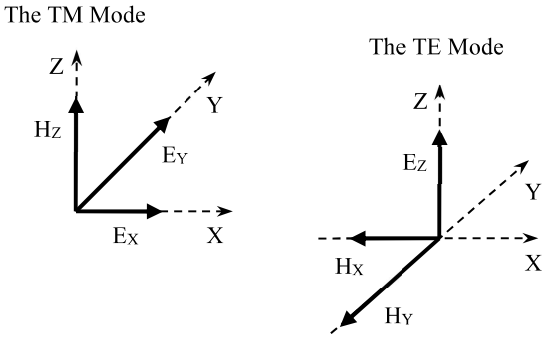

Fig. 2-4. The two evanescent modes with propagation of the phase in X direction and evanescence in Y direction. The physical components (2-16)-(2-17) are represented for $-\pi/4 < \omega t - \phi_X < 0$, i.e. $\cos(\omega t - \phi_X) > 0$ and $\sin(\omega t - \phi_X) < 0$.

The field components of the two evanescent modes are represented in Fig. 2-4, with either E or H in the direction of propagation. The two modes are dual which results from the duality of the Maxwell equations. When χ vanishes they degenerate into the single traveling wave mode. For each mode, the direction of evanescence is any arbitrary direction Y perpendicular to the direction of propagation X. The general solution of the Maxwell Equations is any linear combination of the two modes.

The field components (2-14)-(2-15) can be expressed in any other coordinates, especially in the (x, y, z) coordinates of Fig. 2-3 where (X, Y, Z) are defined with θ, φ, η. For the TM mode (2-14), the magnitudes of E and H components read

$$E_{x0} = \left[-(\cos\varphi\cos\theta\sin\eta + \sin\varphi\cos\eta)\cosh\chi + j\cos\varphi\,\sin\theta\,\sinh\chi\right] Z_0 H_0 \tag{2-18a}$$

$$E_{y0} = \left[(\cos\varphi\cos\eta - \sin\varphi\,\cos\theta\sin\eta)\cosh\chi + j\sin\varphi\,\sin\theta\sinh\chi\right] Z_0 H_0 \tag{2-18b}$$

$$E_{z0} = \left[\sin\theta\sin\eta\,\cosh\chi + j\cos\theta\sinh\chi\right] Z_0 H_0 \tag{2-18c}$$

$$H_{x0} = \left[\sin\varphi\sin\eta - \cos\varphi\cos\theta\cos\eta\right] H_0 \tag{2-18d}$$

$$H_{y0} = -\left[\cos\varphi\sin\eta + \sin\varphi\cos\theta\cos\eta\right] H_0 \tag{2-18e}$$

$$H_{z0} = \sin\theta\cos\eta\; H_0 \tag{2-18f}$$

where H_0 is the magnetic component perpendicular to the direction of propagation and the direction of evanescence. For the TE mode, (2-15) yields

$$E_{x0} = \left[\sin\varphi\sin\eta - \cos\varphi\cos\theta\cos\eta)\right] E_0 \tag{2-19a}$$

$$E_{y0} = -\left[\cos\varphi\sin\eta + \sin\varphi\cos\theta\cos\eta\right] E_0 \tag{2-19b}$$

$$E_{z0} = \sin\theta\cos\eta\; E_0 \tag{2-19c}$$

$$H_{x0} = \left[(\sin\varphi\cos\eta + \cos\varphi\cos\theta\sin\eta)\cosh\chi - j\cos\varphi\sin\theta\sinh\chi\right] E_0 / Z_0 \tag{2-19d}$$

$$H_{y0} = -\left[(\cos\varphi\cos\eta - \sin\varphi\cos\theta\sin\eta)\cosh\chi + j\sin\varphi\sin\theta\sinh\chi\right] E_0 / Z_0 \tag{2-19e}$$

$$H_{z0} = -\left[\sin\theta\sin\eta\cosh\chi + j\cos\theta\sinh\chi\right] E_0 / Z_0 \tag{2-19f}$$

where E_0 is the electric field perpendicular to the direction of propagation and the direction of evanescence.

The expressions of the field components (2-18) and (2-19) are used in section VII for deriving the reflection and transmission coefficients of the evanescent plane waves at interfaces between dielectric media (Fresnel coefficients).

It can be noticed that modes (2-14) and (2-15) are simpler in appearance than the modes in the textbook [5]. This is because they are expressed in the natural coordinates (X, Y, Z) of the waves. It can be shown that (2-14)-(2-15) and the modes in [5] are identical. The derivation of the modes in [5, section 3.2] is a little ambiguous and may be interpreted as only valid in the 2D case. In reality, the modes (2-14) and (2-15), and thus the modes in [5, section 3.2], are the general evanescent plane wave solutions of the Maxwell equations in free space, because the direction Y defined in Fig. 2 is any direction perpendicular to the propagation of the phase. The evanescent plane waves are 2D in nature (the field is invariant in one direction perpendicular to the phase propagation), in the same sense that the pure traveling waves are 1D in nature (the field is invariant in the two directions perpendicular to the phase propagation).

III. The Poynting Vector and the Vectorial Relationships Connecting the E, H, and k Vectors

The Poynting vector gives the flow density of power through a surface. It comes from the Maxwell equations [1, 3, 4] and is thus valid for any kind of plane waves. Using the physical components of the TM mode (2-16) into $\vec{P} = \vec{E} \times \vec{H}$, and assuming without loss of generality that $X = 0$, the Poynting vector is obtained as

$$\vec{P} = \frac{Z_0 H_0^2 A_Y^2}{2}\left[\cosh\chi\,(1 + \cos 2\omega t)\,\vec{u}_X + \sinh\chi\sin 2\omega t\,\vec{u}_Y\right] \tag{3-1}$$

where u_X and u_Y are the unit vectors in directions X and Y. The Poynting vector has a transverse component in the direction of evanescence Y. This component is alternatively positive and negative, and its average value over one period is zero. The average value of the X component is $\frac{1}{2}\, Z_0\, H_0^2\, A_Y^2 \cosh\chi$, which is that of a pure traveling wave of magnitude $H_0\, A_Y$ multiplied with $\cosh\chi$. The average flow of energy of evanescent plane waves is thus in the direction of propagation of the phase X, as with traveling waves, but the instantaneous flow is lying in the (X, Y) plane. The TE mode yields the same P vector as (3-1),

with just E_0^2/ Z_0 in place of $Z_0 H_0^2$. It can be seen that the averages on time of (3-1) and its TE counterpart are identical to the average Poynting vectors given in [5].

Let us now consider the case where the two modes propagate and are evanescent in the same directions *X* and *Y*. The modes are not necessary synchronous which can be expressed by replacing their real magnitudes H_0 and E_0 in (2-14) and (2-15) with $H_0 \exp(j\,\varphi_{TM})$ and $E_0 \exp(j\,\varphi_{TE})$ where φ_{TM} and φ_{TE} are phases with respect with an arbitrary reference. The physical components remain (2-16) and (2-17), with just the argument $(\omega t - \phi_X)$ of the sines and cosines replaced with $(\omega t + \varphi_{TM} - \phi_X)$ in (2-16) and $(\omega t + \varphi_{TE} - \phi_X)$ in (2-17). Denoting as (E_{TM}, H_{TM}) and (E_{TE}, H_{TE}) the modified physical fields of the two modes (2-16) and (2-17), the Poynting vector

$$\vec{P} = (\vec{E}_{TM} + \vec{E}_{TE}) \times (\vec{H}_{TM} + \vec{H}_{TE}) \tag{3-2}$$

can be obtained as:

$$\begin{aligned}\vec{P} = \frac{A_Y^2}{2}\cosh\chi\Big[Z_0 H_0^2\big(1+\cos 2(\omega t+\varphi_{TM})\big) \\ + \frac{E_0^2}{Z_0}\big(1+\cos 2(\omega t+\varphi_{TE})\big)\Big]\vec{u}_X + \frac{A_Y^2}{2}\sinh\chi \\ .\Big[Z_0 H_0^2 \sin 2(\omega t+\varphi_{TM})) + \frac{E_0^2}{Z_0}\sin 2(\omega t+\varphi_{TE})\Big]\vec{u}_Y \\ + A_Y^2 E_0 H_0 \sinh\chi\cosh\chi\sin(\varphi_{TM}-\varphi_{TE})\vec{u}_Z\end{aligned} \tag{3-3}$$

It can be seen that the *X* and *Y* components in (3-3) are the addition of the *P* components of the TM mode (3-1) with those of the TE mode, with their respective phases. However, there is an additional component in *Z* direction which vanishes when $\varphi_{TM} = \varphi_{TE}$, i.e. when the two modes are synchronous. The average flow density of energy over one period reads

$$\begin{aligned}\left\langle\vec{P}\right\rangle = \frac{A_Y^2}{2}\cosh\chi\left[Z_0 H_0^2 + \frac{E_0^2}{Z_0}\right]\vec{u}_X \\ + A_Y^2 E_0 H_0 \sinh\chi\,\cosh\chi\sin(\varphi_{TM}-\varphi_{TE})\vec{u}_Z\end{aligned} \tag{3-4}$$

Thus, when a wave is composed with the two modes whose phases differ with $\Delta\varphi = \varphi_{TM} - \varphi_{TE}$, the average flow of power is not parallel to the propagation of the phase, it is lying in the plane (*X*, *Z*) perpendicular to the direction of evanescence *Y*. Notice that (3-4) can also be derived from the real value of the complex Poynting vector

$$\left\langle\vec{P}\right\rangle = \frac{1}{2}\mathrm{Re}\,al\left[(\vec{E}_{TM}+\vec{E}_{TE})\times(\vec{H}^*_{TM}+\vec{H}^*_{TE})\right] \tag{3-5}$$

using the complex fields (2-14) and (2-15) with magnitudes $H_0 \exp(j\,\varphi_{TM})$ and $E_0 \exp(j\,\varphi_{TE})$.

Let us now consider relationships that connect the *E*, *H*, and *k* vectors of the two modes. Using wavenumbers (2-11) and the TM or TE components (2-14) or (2-15), it can be verified that most relationships that hold with traveling waves also hold with the TM and TE evanescent modes. For instance, for the TM mode, (2-11) and (2-14) yields

$$\vec{k}\times\vec{E} = \left(\frac{\omega}{c}Z_0\cosh^2\chi\,H_0 - \frac{\omega}{c}Z_0\sinh^2\chi\,H_0\right)\vec{u}_Z \tag{3-6}$$

where $\vec{u}_Z$ is the unit vector of Z axis. This gives

$$\vec{k}\times\vec{E} = \omega\mu_0\vec{H} \tag{3-7}$$

Similarly, (2-11) and (2-14) yield

$$\vec{k}\times\vec{H} = -\omega\,\varepsilon_0\vec{E} \tag{3-8}$$

The same relations also hold with the TE mode (2-15). And using (2-11), (2-14), (2-15), it comes

$$\vec{k}\,.\,\vec{E} = 0\,; \qquad \vec{k}\,.\,\vec{H} = 0 \tag{3-9}$$

for the two modes. The *E*, *H*, *k* vectors of the evanescent modes are perpendicular to each other, as the vectors of traveling waves in a vacuum. Since *E* for the TM mode and *H* for the TE mode are not perpendicular to the propagation of the phase, the *k* vector is not parallel to the propagation of the phase, which is also evident from (2-11). The relation of dispersion is obviously the same as with traveling waves, i.e. $\omega = c\,k$, since (2-11) has been obtained as a solution of (2-5).This can be verified using (2-11):

$$\vec{k}\,.\,\vec{k} = k^2 = \frac{\omega^2}{c^2}(\cosh^2\chi - \sinh^2\chi)$$

Notice that relationships (3-7)-(3-9) can also be derived as in [5] from the Maxwell equations, using just the assumption that the waveform is (2-1). Other relations identical to those of traveling waves can be deduced from (2-11), (2-14), (2-15), as the following two for the TM mode and TE mode, respectively:

$$\vec{E}\times\vec{H} = \frac{1}{\varepsilon_0\omega}H_0^2\,\vec{k}\,; \qquad \vec{E}\times\vec{H} = -\frac{1}{\mu_0\omega}E_0^2\,\vec{k} \tag{3-10}$$

Finally, relationships connecting *E*, *H* and the real part of the wave vector $\vec{k}_X$ (2-11) that governs the propagation of the phase can be derived

$$\vec{E} = \frac{1}{\varepsilon_0\omega}\vec{H}\times\vec{k}_X + j\frac{1}{\varepsilon_0\omega}\frac{\sinh\chi}{\cosh\chi}H_0\,\vec{k}_X \tag{3-11}$$

for the TM mode and

$$\vec{H} = -\frac{1}{\mu_0\omega}\vec{E}\times\vec{k}_X - j\frac{1}{\mu_0\omega}\frac{\sinh\chi}{\cosh\chi}E_0\,\vec{k}_X \tag{3-12}$$

for the TE mode. They reduce to (3-7) and (3-8) when $\chi = 0$ (pure traveling waves where $\vec{k} = \vec{k}_X$).

IV. Evanescent Waves with the FDTD Method

This section reports numerical experiments that simulate the propagation of evanescent plane waves (2-10) by means of the full wave FDTD method [7]. To introduce an incident wave in a FDTD grid, a useful and widely used method is the total-field/scattered-field method, also called the Huygens surface method [7]. It consists of enforcing electric current J_S and magnetic current K_S sheets upon a closed surface. J_S and K_S equal in magnitude the *H* and *E* tangential fields that would be produced at the surface location if the incident wave were present. This permits the incident wave to be reproduced in the interior of the surface, whilst no field is produced outside it.

What is done with pure traveling waves can also be done with evanescent plane waves (2-10), for the TM or TE modes (2-14)-(2-15). The implementation is similar to that of traveling waves,

except the presence of an additional component in the direction of propagation, either E_X (2-14a) or H_X(2-15b). Fig. 4-1 depicts a 2D domain with a Huygens surface generating the TM mode propagating in x direction and evanescent in y direction. In that simple case, on the sides C_1-C_2 and C_3-C4 sheet K_S equals the transverse component E_y, because there is no contribution of E_x which is normal to the surface. Conversely, on sides C_2-C_3 and C_4-C_1, only E_x contributes to K_S. At oblique incidence the situation would be a little more complex, the two components would contribute on the whole surface.

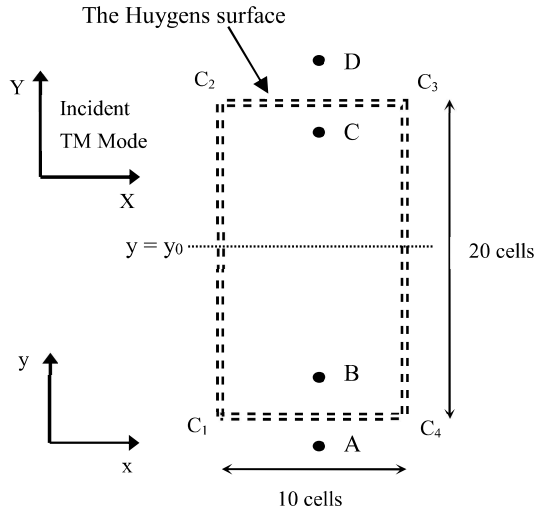

Fig. 4.1. FDTD computational domain for the numerical experiments with evanescent waves ($\Delta x = \Delta y = 5$ cm, $\Delta t = 0.1$ ns). A, B, C, D are the nodes where E_x or E_y are plotted in Figs. 4.2 and 4.3. The incident wave is evanescent in y direction and its phase propagates in x direction.

For a single frequency incident wave, the components E_x, E_y, H_z contributing to K_S and J_S at (x, y) on the Huygens surface in Fig. 4.1 can be expressed as, from (2-16)

$$E_x(x,y,t) = -Z_0\, H_0 \sinh\chi\, e^{-\omega \sinh\chi (y-y_0)/c} \sin\left(\omega t - x\, \omega \cosh\chi / c\right)$$
$$E_y(x,y,t) = Z_0\, H_0 \cosh\chi\, e^{-\omega \sinh\chi (y-y_0)/c} \cos\left(\omega t - x\, \omega \cosh\chi / c\right)$$
$$H_z(x,y,t) = H_0\, e^{-\omega \sinh\chi (y-y_0)/c} \cos\left(\omega t - x\, \omega \cosh\chi / c\right)$$

where y_0 is the ordinate of the middle of the surface (Fig. 4-1) and H_0 is the magnitude of H_z at $y = y_0$ ($H_0 = 100/Z_0$ A/m in the calculations). In the experiment reported in Fig. 4-2, the period of the wave was 50 time steps Δt and its magnitude was growing from 0 to H_0 over 10 periods to obtain a frequency content as close as possible to a single frequency wave.

The calculated E_x and E_y components are plotted in Fig. 4-2, at several locations inside and outside the Huygens surface, when the steady state has been obtained. The calculation was performed with $\cosh\chi = 1.03$, i.e. $\sinh\chi = 0.24678$. We can note that the $\pi/2$ advance of E_x with respect to E_y is well reproduced. The magnitude of E_x and E_y are smaller at point C than at point B, because the wave is evanescent in $+y$ direction. The ratios of the fields at B and C agree well with the $\exp[-\omega/c\, \sinh\chi\, (y\text{-}y_0)]$ evanescence. For example, the FDTD ratio of E_y at B and C is 0.4150 while its theoretical value for the 17 cells separating the two nodes is 0.4155. Similarly, the ratio of the FDTD magnitudes of E_y and E_x at point B is 0.2286, in acceptable accordance with the theoretical value $\sinh\chi/\cosh\chi = 0.2396$ (due to the staggered FDTD grid, E_x in Fig. 4-2 is the average of values at the two nodes located $\Delta y/2$ from the E_y node). Outside the Huygens surface, the field leakage is small, as illustrated with points A and D. It is larger than with pure traveling waves and grows with $\cosh\chi$. In this experiment it was about 2 % of the field inside the surface.

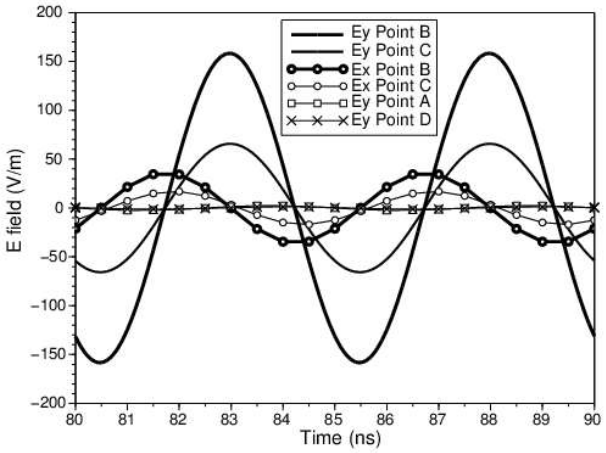

Fig. 4-2. Electric field inside and outside a Huygens surface generating a sinusoidal TM evanescent field. The locations of points A, B, C, D are shown in Fig. 4-1.

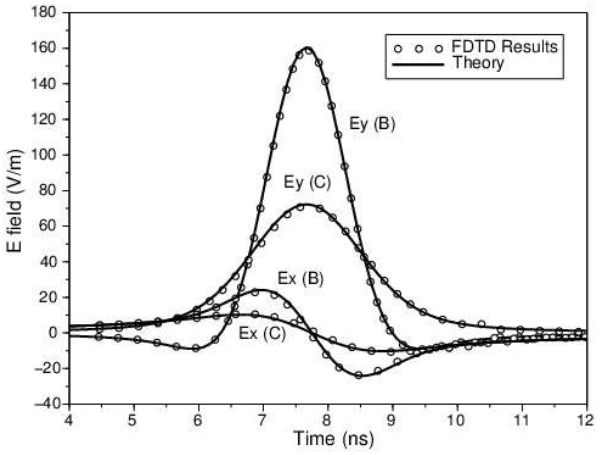

Fig. 4-3. E_x and E_y fields inside the Huygens surface at B and C locations in Fig. 4.1. The incident waveform at $y = y_0$ is a Gaussian function. The FDTD results (circles) are compared with the theoretical field (continuous lines).

Beside the above pure sinusoidal wave, it is also possible to implement time domain incident waves. Denoting as $S(\omega)$ the spectrum of the desired waveform at a location (x_0, y_0), the spectrum of the field at ordinate y reads, in the case of Fig. 4-1 where the evanescence is in y direction

$$E_x(x_0,,y,\omega) = j Z_0\, H_0 \sinh\chi\, S(\omega)\, e^{-\omega \sinh\chi (y-y_0)/c} \qquad (4\text{-}1a)$$
$$E_y(x_0,,y,\omega) = Z_0\, H_0 \cosh\chi\, S(\omega)\, e^{-\omega \sinh\chi (y-y_0)/c} \qquad (4\text{-}1b)$$
$$H_z(x_0,,y,\omega) = H_0\, S(\omega)\, e^{-\omega \sinh\chi (y-y_0)/c} \qquad (4\text{-}1c)$$

The time domain field at (x_0, y) can be obtained by the Inverse Fourier transform of (4-1). This field can then be propagated in x direction with the phase celerity $c/\cosh\chi$ to obtain the contributions to J_S and K_S at any (x, y) on the Huygens surface. Such a time domain incident wave has been implemented with a Gaussian pulse in the 2D case in Fig. 4-1.

Results of an experiment with an incident wave of $\cosh\chi$ = 1.03 are reported in Fig. 4-3. The incident pulse at $y = y_0$ was the Gaussian pulse of spectrum

$$S(\omega) = \frac{1}{T\sqrt{\pi}} e^{-(\omega T/2)^2} \tag{4-2}$$

with T = 1 ns. The FDTD fields E_x and E_y at locations B and C in Fig. 4-1 are compared with the theoretical E_x and E_y computed by the inverse Fourier transforms of (4-1a) and (4-1b). As can be observed, the FDTD field inside the Huygens surface is in good agreement with the theoretical field.

Finally, the simple experiments in Figs. 4-1 to 4-3 show that evanescent plane waves can be generated in a FDTD grid by means of the usual Huygens surface method, and demonstrates that such waves can propagate in the FDTD grid in accordance with theory.

V. Evanescent Plane Waves in some Problems

In many problems of electromagnetism, the analytical solution can be interpreted as a set of plane waves. This is well documented in textbooks when the solution is propagative, i.e. not evanescent. This is the case in waveguiding structures where the electromagnetic energy of each mode can propagate without attenuation above the cutoff frequency. In that regime, the field is a set of traveling plane waves. Below the cutoff, the modes are evanescent and can also be interpreted as a set of plane waves, more precisely a set of evanescent plane waves. In the following we address the cases of parallel plate waveguides and rectangular waveguides, where the solution is a set of two or four evanescent waves (2-14) or (2-15). Another example is also addressed, namely the field reflected from corrugated surfaces also composed with evanescent plane waves.

The simplest waveguide, depicted in Fig. 5-1, is composed with two parallel plates. For the transverse electric (TE) modes [3], the E (x, y, t) field is parallel to the plates and in the form

$$E_z = E_0 \sin\left(\frac{m\pi}{a}x\right) e^{-jk_z y} \tag{5-1}$$

where the time dependence $\exp(j\omega t)$ has been omitted, m is an integer, and

$$k_y = \pm\sqrt{\frac{\omega^2}{c^2} - \frac{m^2\pi^2}{a^2}} \tag{5-2}$$

Below the cutoff angular frequency $\omega_c = m\,\pi\,c/a$, the quantity under the square root is negative and (5-1) becomes:

$$E_z = E_0 \sin\left(\frac{m\pi}{a}x\right) e^{-\sqrt{\frac{m^2\pi^2}{a^2} - \frac{\omega^2}{c^2}}\,y} \tag{5-3}$$

This wave is evanescent in y direction of the waveguide. Replacing the sine with exponentials, (5-3) becomes

$$E_z = \frac{E_0}{2j}\left[e^{j\frac{m\pi}{a}x} e^{-\sqrt{\frac{m^2\pi^2}{a^2} - \frac{\omega^2}{c^2}}\,y} - e^{-j\frac{m\pi}{a}x} e^{-\sqrt{\frac{m^2\pi^2}{a^2} - \frac{\omega^2}{c^2}}\,y} \right] \tag{5-4}$$

where quantities within the bracket can be viewed as two waves E_{z1} and E_{z2} with phases propagating in $-x$ and $+x$ directions, and magnitudes decreasing in y direction. Thus, the field E_z is the addition of two plane waves whose magnitudes are not uniform in the plane perpendicular to their propagation.

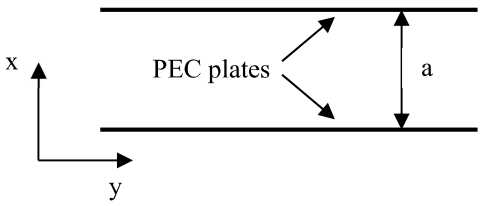

Fig. 5-1. A parallel plate waveguide.

Defining now an hyperbolic cosine $\cosh\chi$ as

$$\cosh\chi = \frac{m\pi c}{\omega a} \tag{5-5}$$

and using $\cosh^2\chi - \sinh^2\chi = 1$, the second plane waves in (5-4), can be rewritten as

$$E_{z2} = \frac{jE_0}{2} e^{-j\frac{\omega}{c}\cosh\chi\, x} e^{-\frac{\omega}{c}\sinh\chi\, y} \tag{5-6}$$

This is the waveform (2-10) of a plane wave propagating in direction x and evanescent in direction y. Using (5-6) into the Maxwell equations and taking account of the invariance in z direction, two H components are obtained as

$$H_{x2} = -j/Z_0 \sinh\chi\, E_{z2} \tag{5-7a}$$

$$H_{y2} = -1/Z_0 \cosh\chi\, E_{z2} \tag{5-7b}$$

which are parallel and perpendicular, respectively, to the direction of propagation x, with same ratios H_{x2} / E_{z2} and H_{y2} / E_{z2} as with the TE mode (2-15). In brief, the second wave in (5-4) is the TE mode (2-15). Similar expressions hold for the first wave, with just a positive sign in the exponential of the phase in (5-6). Finally, below the cutoff frequency, the TE mode in the waveguide is a set of two TE evanescent plane waves (2-15).

Let us now address the case of a z-directed rectangular waveguide (Fig. 5-2) of section (a, b) in the plane (x, y). And let us consider the component E_y of the TE mode (m, n). It is known it can be written as

$$E_y = E_{mn} \sin\left(\frac{m\pi}{a}x\right) \cos\left(\frac{m\pi}{b}y\right) e^{jk_z z} \tag{5-8a}$$

where:

$$k_z = \pm\sqrt{\frac{\omega^2}{c^2} - \frac{m^2\pi^2}{a^2} - \frac{n^2\pi^2}{b^2}} \tag{5-8b}$$

Below the cutoff ω_c that renders the quantity under the square root negative in (5-8b), (5-8a) can be rewritten as

$$E_y = \frac{E_{mn}}{4j}\frac{m}{a}\left[e^{j\pi\left(\frac{m}{a}x + \frac{n}{b}y\right)} e^{-\Theta z} + e^{j\pi\left(\frac{m}{a}x - \frac{n}{b}y\right)} e^{-\Theta z} \right.$$

$$-e^{j\pi\left(-\frac{m}{a}x+\frac{n}{b}y\right)}e^{-\Theta z}-e^{j\pi\left(-\frac{m}{a}x-\frac{n}{b}y\right)}e^{-\Theta z}\Big] \qquad (5\text{-}9)$$

where:

$$\Theta=\sqrt{\frac{m^2\pi^2}{a^2}+\frac{n^2\pi^2}{b^2}-\frac{\omega^2}{c^2}} \qquad (5\text{-}10)$$

The four terms in the bracket of (5-9) can be interpreted as four plane waves evanescent in z direction, with their phase propagating in the (x, y) plane. Consider for instance the fourth wave. Its phase propagates in direction θ with respect with the x axis with

$$\tan\theta=\frac{n\,a}{m\,b} \qquad (5\text{-}11)$$

Denoting as X this direction of propagation, the fourth wave can be rewritten as

$$E_{y4}=\frac{j\,E_{mn}}{4}\frac{m}{a}e^{-j\pi\sqrt{\frac{m^2}{a^2}+\frac{n^2}{b^2}}X}\;e^{-\Theta z} \qquad (5\text{-}12)$$

Similarly, the other three waves in (5-9) propagate in directions π–θ, π+θ, and -θ. Defining now an hyperbolic cosine as

$$\cosh\chi=\frac{\pi\,c}{\omega}\sqrt{\frac{m^2}{a^2}+\frac{n^2}{b^2}} \qquad (5\text{-}13)$$

the wave (5-12) can be rewritten as

$$E_{y4}=\frac{j\,E_{mn}}{4}\frac{m}{a}e^{-j\frac{\omega}{c}\cosh\chi\,X}\;e^{-\frac{\omega}{c}\sinh\chi\,z} \qquad (5\text{-}14)$$

which is nothing but the waveform (2-10) of an evanescent plane wave.

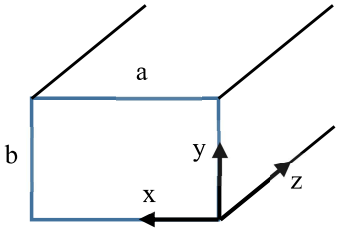

Fig. 5-2. A rectangular waveguide.

Concerning the other components of the TE mode, it can be seen that E_x just differs from E_y with factor -n/b in place of m/a in (5-9) and (5-14), which means that the resulting $E_{x\text{-}y}$ field is perpendicular to the direction of propagation θ (5-11). And components H_x and H_y just differ with factors m/a and n/b, which means that the resulting $H_{x\text{-}y}$ is parallel to the direction θ. Thus, the situation is that of the TE mode (2-15), with a magnetic component $H_{x\text{-}y}$ in the direction of propagation, an electric component $E_{x\text{-}y}$ perpendicular to the propagation and to the direction of evanescence z, and with a component H_z in the direction of evanescence. Concerning the magnitudes of the field components, it can be shown that the ratios $H_z/E_{x\text{-}y}$ and $H_{x\text{-}y}/E_{x\text{-}y}$ agree with the ratio of components of (2-15). From which the fourth wave in (5-9) is a TE plane wave (2-15). This also holds for the other three waves in (5-9). In conclusion, the evanescent fields in the waveguide can be expressed as a set of four evanescent TE plane waves in the form (2-15) where Y is the longitudinal direction z of the waveguide, and X and Z are directions lying in the transverse plane. The evanescence parameter χ (5-13) depends on the sizes of the waveguide (a, b) and on the mode (m, n). The same interpretation in term of evanescent plane waves also holds with the TM modes.

Let us now briefly consider another problem where evanescent waves are present, the reflection by periodic corrugated surfaces addressed in [3]. The reflected field is expressed as an infinite sum of Floquet modes. At low frequency, when the wavelength is larger than the period of the corrugations, the modes are evanescent in the direction x perpendicular to the surface. In that case, mode n can be expressed in the form [3]

$$H_y=H_n e^{-j\left(\frac{\omega}{c}\sin\theta+n\frac{\pi}{b}\right)z}\;e^{-\sqrt{\left(\frac{\omega}{c}\sin\theta+n\frac{\pi}{b}\right)^2-\frac{\omega^2}{c^2}}\,x} \qquad (5\text{-}15)$$

where 2 b is the period and θ is the angle of incidence of the wave. Defining

$$\cosh\chi=\sin\theta+\frac{n\pi c}{\omega b} \qquad (5\text{-}16)$$

the mode can be rewritten as

$$H_y=H_n e^{-j\frac{\omega}{c}\cosh\chi\,z}\;e^{-\frac{\omega}{c}\sinh\chi\,x} \qquad (5\text{-}17)$$

which is the waveform (2-10). Thus, the Floquet modes are non uniform plane waves evanescent in direction x perpendicular to the surface and propagating in direction z parallel to the surface.

In summary, the evanescent fields present in waveguides and on corrugated surfaces can be viewed as sets of TM or TE evanescent plane wave solutions of Maxwell equations in free space (2-14)-(2-15).

VI. The Snell Law of the Evanescent Waves

In this section and in the next one we address the question of the reflection and transmission of an incident evanescent wave at an interface between two media. In the above, it has been assumed that the medium is a vacuum. However, the results are valid as well with a dielectric medium, with just ε in place of ε_0 (and the corresponding velocity or impedance in place of c or Z_0). Let us now consider an interface perpendicular to direction z separating two media where $c = c_1$ and $c = c_2$ (Fig. 6-1). The incident wave propagates in direction (θ_1, φ_1), its direction of evanescence is η_1, and its evanescence coefficient χ_1. The parameters of the reflected wave are denoted as θ_r, φ_r, η_r, χ_r, and those of the transmitted wave as θ_2, φ_2, η_2, χ_2.

Let us first address the reflection from the interface. The phases of the reflected and incident waves must be equal in the interface, that is $k_{xr} = k_{x1}$ and $k_{yr} = k_{y1}$. Using (2-12a) and (2-12b), we obtain two equations with real and imaginary parts. They are equivalent to a set of four real equations for the four unknowns θ_r, φ_r, η_r, χ_r:

$$\cosh\chi_r\cos\varphi_r\sin\theta_r=\cosh\chi_1\cos\varphi_1\sin\theta_1 \qquad (6\text{-}1a)$$

$$\sinh\chi_r\cos\varphi_r\cos\theta_r\sin\eta_r+\sinh\chi_r\sin\varphi_r\cos\eta_r$$
$$=\sinh\chi_1\cos\varphi_1\cos\theta_1\sin\eta_1+\sinh\chi_1\sin\varphi_1\cos\eta_1 \qquad (6\text{-}1b)$$

$$\cosh\chi_r\sin\varphi_r\sin\theta_r=\cosh\chi_1\sin\varphi_1\sin\theta_1 \qquad (6\text{-}1c)$$

$$\sinh\chi_r \sin\varphi_r \cos\theta_r \sin\eta_r - \sinh\chi_r \cos\varphi_r \cos\eta_r$$
$$= \sinh\chi_1 \sin\varphi_1 \cos\theta_1 \sin\eta_1 - \sinh\chi_1 \cos\varphi_1 \cos\eta_1 \quad (6\text{-}1d)$$

It can be verified that the following solution satisfies (6-1)

$$\theta_r = \pi - \theta_1 \quad (6\text{-}2a)$$
$$\varphi_r = \varphi_1 \quad (6\text{-}2b)$$
$$\eta_r = \pi - \eta_1 \quad (6\text{-}2c)$$
$$\chi_r = -\chi_1 \quad (6\text{-}2d)$$

where (6-2a) and (6-2b) are the same as in the case of a uniform wave. The magnitude of the evanescence coefficient χ is left unchanged, only its sign is changed, which allows the direction of evanescence of the incident and reflected waves to be the same.

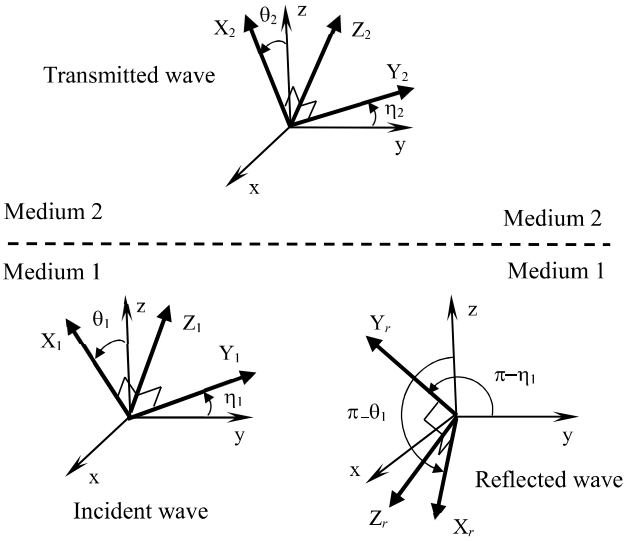

Fig. 6-1. The incident, reflected, and transmitted waves at an interface perpendicular to direction *z*. The direction of propagation of the incident wave X_1 is θ_1 from *z* axis and its direction of evanescence Y_1 is η_1 from *y* axis (it is assumed without loss of generality that $\varphi = 0$). From Fig. 2.3 and (6-2c), the direction of evanescence Y_r of the reflected wave is obtained by a rotation π-η_1 of *y* axis around X_r axis (*y*' in Fig. 2.3 is *y* here since $\varphi = 0$).

Let us now consider the transmission through the interface. Using (2-12b) and writing that $k_{y2} = k_{y1}$ in the interface yields a complex equation whose real part reads

$$\cosh\chi_2 \sin\varphi_2 \sin\theta_2 = (c_2/c_1)\cosh\chi_1 \sin\varphi_1 \sin\theta_1$$

It shows that $\varphi_2 = 0$ if $\varphi_1 = 0$. Since any situation of the incident wave with respect to the interface can be expressed in coordinates where $\varphi_1 = 0$, it can be assumed that $\varphi_1 = \varphi_2 = 0$ without loss of generality. Writing then that $k_{x2} = k_{x1}$ and $k_{y2} = k_{y1}$ and using (2-12), the following three equations are obtained:

$$A = \cosh\chi_2 \sin\theta_2 = (c_2/c_1)\cosh\chi_1 \sin\theta_1 \quad (6\text{-}3a)$$
$$B = \sinh\chi_2 \cos\theta_2 \sin\eta_2 = (c_2/c_1)\sinh\chi_1 \cos\theta_1 \sin\eta_1 \quad (6\text{-}3b)$$
$$C = \sinh\chi_2 \cos\eta_2 = (c_2/c_1)\sinh\chi_1 \cos\eta_1 \quad (6\text{-}3c)$$

The three unknowns θ_2, η_2, χ_2 can be found from this set of three equations. For example, $\sin\theta_2$ and $\sinh\chi 2$ can be found as

$$\sin\theta_2 = \sqrt{\frac{1+D^2-\sqrt{(1+D^2)^2-4(1+C^2)A^2}}{2(1+C^2)}} \quad (6\text{-}4)$$

$$\sinh\chi_2 = \sqrt{\frac{D^2-1+\sqrt{(D^2-1)^2-4(A^2C^2-B^2-C^2)}}{2}} \quad (6\text{-}5)$$

where $D^2 = A^2+B^2+C^2$. Then, $\cos\eta_2$ can be obtained from (6-3c) as

$$\cos\eta_2 = (c_2/c_1)\sinh\chi_1 \cos\eta_1 / \sinh\chi_2 \quad (6\text{-}6)$$

It can be shown that the quantities under the square roots in (6-4) and (6-5) are always positive, so that (6-4) and (6-5) are valid with any set c_1, c_2, θ_1, η_1, χ_1. Equation (6-4) always yields $\sin\theta_2 \le 1$, even in the case of total reflection where $\theta_2 = \pi/2$ (see next section). In summary, equations (6-4)-(6-6) are the Snell law of the evanescent plane waves.

VII. The Fresnel Coefficients

The reflection and transmission coefficients at an interface can be derived as with uniform plane waves, by enforcing the continuity of the tangential components of *E* and *H*. Here, because of the evanescence in direction η_1 and the presence of a component of *E* or *H* in the direction of propagation, there are four components lying in the interface, even with a pure TM (2-14) or TE (2-15) incident mode (except with special values of η or θ). This results in four equations of continuity, instead of two with uniform TE or TM plane waves. In consequence, the continuity cannot be satisfied by a single mode, which means that an incident mode yields reflected and transmitted energy into the other mode. To derive the reflection and transmission coefficients, let us assume the incident wave is the addition of the two modes (2-14) and (2-15), with magnitudes H_{0i} and E_{0i}, respectively. And let us denote as H_{0r} and E_{0r} the magnitudes of the reflected modes, and H_{0t} and E_{0t} the magnitudes of the transmitted modes. Using then the components of the field (2-18)-(2-19) with $\varphi_1 = \varphi_2 = 0$, and taking account of (6-2) which in particular means that $\cos\theta_r = -\cos\theta_1$ and $\cos\eta_r = -\cos\eta_1$, the continuity of E_x, E_y, H_x, H_y in the interface yields the following four equations:

$$(\cos\theta_1 \sin\eta_1 \cosh\chi_1 - j\sin\theta_1 \sinh\chi_1) Z_1 (H_{0i} - H_{0r})$$
$$+ \cos\theta_1 \cos\eta_1 (E_{0i} + E_{0r}) = \cos\theta_2 \cos\eta_2 E_{0t}$$
$$+ (\cos\theta_2 \sin\eta_2 \cosh\chi_2 - j\sin\theta_2 \sinh\chi_2) Z_2 H_{0t} \quad (7\text{-}1a)$$

$$\cos\eta_1 \cosh\chi_1 Z_1 (H_{0i} - H_{0r}) - \sin\eta_1 (E_{0i} + E_{0r})$$
$$= \cos\eta_2 \cosh\chi_2 Z_2 H_{0t} - \sin\eta_2 E_{0t} \quad (7\text{-}1b)$$

$$(\cos\theta_1 \sin\eta_1 \cosh\chi_1 - j\sin\theta_1 \sinh\chi_1)(E_{0i} - E_{0r})/Z_1$$
$$- \cos\theta_1 \cos\eta_1 (H_{0i} + H_{0r}) = -\cos\theta_2 \cos\eta_2 H_{0t}$$
$$+ (\cos\theta_2 \sin\eta_2 \cosh\chi_2 - j\sin\theta_2 \sinh\chi_2) E_{0t}/Z_2 \quad (7\text{-}1c)$$

$$\sin\eta_1 (H_{0i} + H_{0r}) + \cos\eta_1 \cosh\chi_1 (E_{0i} - E_{0r})/Z_1$$
$$= \sin\eta_2 H_{0t} + \cos\eta_2 \cosh\chi_2 E_{0t}/Z_2 \quad (7\text{-}1d)$$

Let us then express the four unknowns H_{0r}, E_{0r}, H_{0t}, E_{0t} of the linear system (7-1) in function of the incident magnitudes H_{0i} and E_{0i} as

$$H_{0r} = r_{hh} H_{0i} + r_{eh} E_{0i} \tag{7-2a}$$

$$E_{0r} = r_{he} H_{0i} + r_{ee} E_{0i} \tag{7-2a}$$

$$H_{0t} = t_{hh} H_{0i} + t_{eh} E_{0i} \tag{7-2a}$$

$$E_{0t} = t_{he} H_{0i} + t_{ee} E_{0i} \tag{7-2a}$$

The coefficients r and t in (7-2) can then be found by solving two times (7-1), one time with $H_{0i} = 1$ and $E_{0i} = 0$ yields r_{hh}, r_{he}, t_{hh}, t_{he}, and one time with $H_{0i} = 0$ and $E_{0i} = 1$ yields r_{eh}, r_{ee}, t_{eh}, t_{ee}. The following reflection and transmission coefficients are obtained

$$\begin{pmatrix} r_{hh} \\ r_{he} \\ t_{hh} \\ t_{he} \end{pmatrix} = M^{-1} \begin{pmatrix} U_1 Z_1 \\ W_1 Z_1 \\ \sin\eta_1 \\ -V_1 \end{pmatrix} \quad \text{and} \quad \begin{pmatrix} r_{eh} \\ r_{ee} \\ t_{eh} \\ t_{ee} \end{pmatrix} = M^{-1} \begin{pmatrix} -\sin\eta_1 \\ V_1 \\ U_1 / Z_1 \\ W_1 / Z_1 \end{pmatrix} \tag{7-3}$$

where matrix M and quantities U_m, V_m, W_m read

$$M = \begin{pmatrix} U_1 Z_1 & \sin\eta_1 & U_2 Z_2 & -\sin\eta_2 \\ W_1 Z_1 & -V_1 & W_2 Z_2 & V_2 \\ -\sin\eta_1 & U_1 / Z_1 & \sin\eta_2 & U_2 / Z_2 \\ V_1 & W_1 / Z_1 & -V_2 & W_2 / Z_2 \end{pmatrix} \tag{7-4}$$

$$U_m = \cosh\chi_m \cos\eta_m \quad ; \quad V_m = \cos\theta_m \cos\eta_m \tag{7-5}$$

$$W_m = \cosh\chi_m \cos\theta_m \sin\eta_m - j \sinh\chi_m \sin\theta_m \tag{7-6}$$

The two solutions (7-3) could be explicitly expressed in algebraic form. However, it is simpler to compute them numerically, after replacement of the trigonometric and hyperbolic functions of θ_2, χ_2, η_2 with their numerical values from the Snell law (6-4)-(6-6). The coefficients plotted in Fig. 7-2 have been obtained by this method.

In the following, three special cases where the system is simpler are addressed and discussed.

The special case where the evanescence is in the plane of incidence ($\eta_1 = \pm 90°$)

Let us first consider the special case where $\eta_1 = \pi/2$, which means that the direction of evanescence Y_1 is lying in the plane of incidence (the plane perpendicular to the interface where the direction of propagation X_1 is lying). Equation (6-3c) yields $C = 0$ and $\eta_2 = \pi/2$. System (7-1) then reduces to

$$C_w(\chi_1,\theta_1) Z_1 (H_{0i} - H_{0r}) = C_w(\chi_2,\theta_2) Z_2 H_{0t} \tag{7-7a}$$

$$E_{0i} + E_{0r} = E_{0t} \tag{7-7b}$$

$$C_w(\chi_1,\theta_1) (E_{0i} - E_{0r}) / Z_1 = C_w(\chi_2,\theta_2) E_{0t} / Z_2 \tag{7-7c}$$

$$H_{0i} + H_{0r} = H_{0t} \tag{7-7d}$$

where $C_w(\chi,\theta)$ is the special case $\eta = \pi/2$ of (7-6):

$$C_w(\chi,\theta) = \cosh\chi \cos\theta - j \sinh\chi \sin\theta \tag{7-8}$$

System (7-7) is composed with two independent subsets, (7-7a)-(7-7d), and (7-7b)-(7-7c), respectively. It means that the two modes are decoupled, i.e. $r_{he} = r_{eh} = t_{he} = t_{eh} = 0$. This was expected because with the two modes the projections of the E and H fields in the interface reduce to only one E component and one H component, with the projections of the TE mode perpendicular to those of the TM mode. The two modes are thus independent. System (7-7) yields the coefficients

$$r_{hh} = \frac{Z_1 C_w(\chi_1,\theta_1) - Z_2 C_w(\chi_2,\theta_2)}{Z_1 C_w(\chi_1,\theta_1) + Z_2 C_w(\chi_2,\theta_2)} \tag{7-9a}$$

$$r_{ee} = \frac{Z_2 C_w(\chi_1,\theta_1) - Z_1 C_w(\chi_2,\theta_2)}{Z_2 C_w(\chi_1,\theta_1) + Z_1 C_w(\chi_2,\theta_2)} \tag{7-9b}$$

with in addition $t_{hh} = 1 + r_{hh}$ and $t_{ee} = 1 + r_{ee}$. Quantity $C_w(\chi_2, \theta_2)$ can be found using (6-4) and (6-5). It can also be obtained by means of

$$C_w(\chi_2,\theta_2) = \left[1 - \left(\frac{c_2}{c_1}\right)^2 (\cosh\chi_1 \sin\theta_1 + j \sinh\chi_1 \cos\theta_1)^2\right]^{1/2} \tag{7-10}$$

which can be derived using $k_{x1} = k_{x2}$, with k_x from (2-12a).

In the case $\eta_1 = -\pi/2$, (7-7)-(7-10) remain valid with just the change of the sign in front of j in (7-8) and (7-10). The reflections (7-9) of the cases $\eta_1 = \pi/2$ and $\eta_1 = -\pi/2$ are complex conjugates.

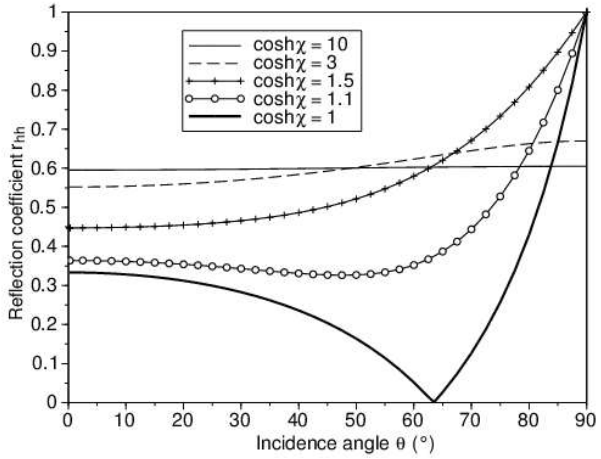

Fig. 7-1. Reflection coefficient r_{hh} in the case where the direction of evanescence is in the plane of incidence ($\eta_1 = \pm 90°$). The interface is between a vacuum and a dielectric of $\varepsilon_r = 4$. The case $\cosh\chi = 1$ corresponds to a traveling wave of reflection coefficient r_p. There is no conversion of energy from the TM mode to the TE mode ($r_{he} = 0$ for any $\cosh\chi$).

Reflection r_{hh} (7-9a) from the interface between a vacuum and a dielectric of $\varepsilon_r = 4$ (i.e. $c_1/c_2 = Z_1/Z_2 = 2$) is plotted in Fig. 7-1 for several evanescence coefficients $\cosh\chi$. In the case $\cosh\chi = 1$ the incident wave is a pure traveling wave with the E field parallel to the plane of incidence. Its reflection coefficient is the r_p coefficient of traveling waves in textbooks.

It can be noticed that the TM mode in the 3D case $\eta_1 = -\pi/2$ is nothing but the 2D case considered in a PML medium in [6].

The special case where the evanescence is perpendicular to the plane of incidence ($\eta_1 = 0$)

Let us now briefly consider the case where $\eta_1 = 0$. Equation (6-3b) shows that $B = 0$ and $\eta_2 = 0$. Using $\eta_1 = \eta_2 = 0$ in (7-1) results in a simpler system where the terms with *sin*η are missing, but there remains two equations involving the two modes, namely (7-1a) and (7-1c). The modes are thus coupled at the interface, and the algebraic expressions of the eight coefficients (7-2) would remain complicated. As in the general case, a numerical solution is simpler. We can just note that in this special case the calculation of χ_2 and θ_2 is quite simple, since (6-3c) yields $\sinh\chi_2 = C$ and then from (6-3a) $\sin\theta_2 = A/(1+C^2)^{1/2}$ which can also be obtained with $B = 0$ in (6-4).

The reflections r_{hh} and r_{he}, computed by solving numerically system (7-3) are plotted in Fig. 7-2 for a vacuum-dielectric interface ($\varepsilon_r = 4$). For the traveling wave case ($\cosh\chi = 1$) the reflection r_{hh} is the coefficient r_s in textbooks and $r_{he} = 0$. For evanescent waves, part of the energy of the TM incident mode is reflected into the TE mode (red coefficients r_{he} in the figure).

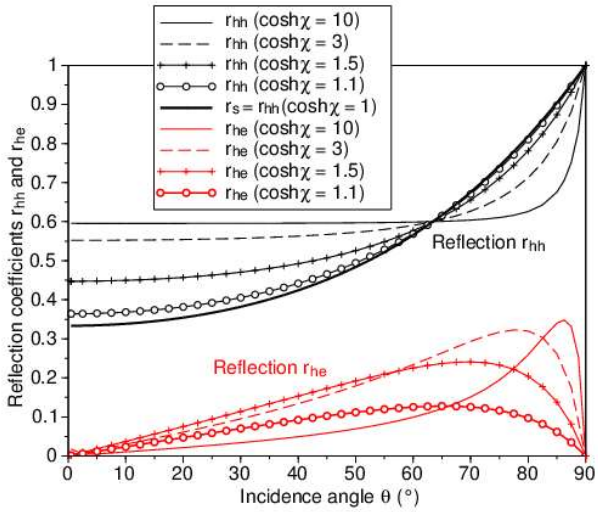

Fig. 7-2. Reflection coefficients r_{hh} and r_{he} when the direction of evanescence is perpendicular to the plane of incidence ($\eta_1 = 0$). The interface is between a vacuum and a dielectric of $\varepsilon_r = 4$. The case $\cosh\chi = 1$ corresponds to a traveling wave of reflection coefficient r_s (in that case $r_{he} = 0$). For evanescent waves ($\cosh\chi > 1$), part of the energy of the TM mode is converted into the TE mode (red curves).

The special case where the reflection is total

We now consider a case well known in Optics, namely the evanescent wave existing behind the interface between two dielectric media in the case of total reflection. Let be media 1 and 2 with speeds c_1 and c_2 such that $c_2 > c_1$. And let be a non evanescent incident wave, which means $\chi_1 = 0$. The reflected wave is non evanescent (since $\chi_r = -\chi_1 = 0$) and equations (6-3) become

$$\cosh\chi_2 \sin\theta_2 = (c_2/c_1)\ \sin\theta_1 = A \qquad (7\text{-}11a)$$

$$\sinh\chi_2 \cos\theta_2 \sin\eta_2 = 0 \qquad (7\text{-}11b)$$

$$\sinh\chi_2 \cos\eta_2 = 0 \qquad (7\text{-}11c)$$

For θ such that $c_2/c_1 \sin\theta_1 > 1$, (7-11a) can be satisfied only if $\cosh\chi_2 > 1$, i.e. if $\chi_2 \neq 0$. In consequence, (7-11c) implies that $\eta_2 = \pm\ \pi/2$ and then (7-11b) that $\theta_2 = \pm\ \pi/2$. Thus, the transmitted wave is evanescent with

$$\cosh\chi_2 = c_2/c_1\ \sin\theta_1 \qquad (7\text{-}12)$$

Notice that χ_2, θ_2, η_2, can also be obtained using (6-4)-(6-6). Especially, equation (6-4) gives $\sin\theta_2 = 1$ since $B = C = 0$ and $A > 1$ (the inner square root reduces to A^2-1). With $\theta_2 = \eta_2 = \pi/2$, $\varphi_2 = 0$, and (7-12), the wave vector (2-12) yields $k_{y2} = 0$ and

$$k_{x2} = \frac{\omega}{c_2}\frac{c_2}{c_1}\sin\theta_1 \qquad (7\text{-}13a)$$

$$k_{z2} = -\frac{\omega}{c_2} j\sqrt{(c_2/c_1)^2\sin^2\theta_1 - 1} \qquad (7\text{-}13b)$$

from which the transmitted waveform reads

$$\psi(x,z) = e^{-j\frac{\omega}{c_1}\sin\theta_1 x}\ e^{-\frac{\omega}{c_2}\sqrt{(c_2/c_1)^2\sin^2\theta_1 - 1}\ z} \qquad (7\text{-}14)$$

This wave propagates in direction x parallel to the interface and is evanescent in direction z perpendicular to the interface. The reflection coefficient can be found using (7-1). Since the incident wave is non evanescent, the angle η_1 is arbitrary. With $\eta_1 = \pm\ \pi/2$ the degenerated (since $\sinh\chi_1 = 0$) TM and TE modes correspond to E fields parallel and perpendicular, respectively, to the plane of incidence. Using $\eta_1 = \pi/2$ along with $\chi_1 = 0$ and $\theta_2 = \eta_2 = \pi/2$ into (7-1) yields two subsets of two equations. The two modes are decoupled. The following reflection coefficient r_{hh} can be deduced as

$$r_{hh} = \frac{Z_1\cos\theta_1 + jZ_2\sqrt{(c_2/c_1)^2\sin^2\theta_1 - 1}}{Z_1\cos\theta_1 - jZ_2\sqrt{(c_2/c_1)^2\sin^2\theta_1 - 1}} \qquad (7\text{-}15)$$

The same formula applies for r_{ee} with just permutation of Z_1 with Z_2. As expected, the reflection is total since the modulus of (7-15) equals one. Equations (7-14) and (7-15) can be found in textbooks on Optics. Using $\eta_1 = -\pi/2$, the reflections r_{hh} and r_{ee} would be the complex conjugates of those obtained with $\eta_1 = +\pi/2$.

Conservation of energy through the interface

The average flow density of power that flows from medium 1 through the interface must equal the average flow density of power of the wave transmitted into medium 2. More precisely, the $< P_z >$ components normal to the interface in media 1 and 2 must be equal. In general, the transmitted wave is composed with the two modes that propagate and are evanescent in the same directions. The corresponding flow can be computed using (3-4) which yields, in the case of an incident TM mode:

$$\langle P_{z2}\rangle = \frac{1}{2}\cosh\chi_2\ H_0^2\left[Z_2|t_{hh}|^2 + \frac{|t_{he}|^2}{Z_2}\right]\cos\theta_2 + H_0^2|t_{hh}||t_{he}|\ \sinh\chi_2\ \cosh\chi_2\sin(\Delta\varphi)\ \cos\eta_2\sin\theta_2 \qquad (7\text{-}16)$$

where it is assumed without loss of generality that $A_Y = 1$, and where Δφ is the difference of the phases of the transmission coefficients t_{hh} and t_{he}. Concerning the energy flow $< P_{z1} >$ in

medium 1 the situation is more complex since there are three modes: the incident wave, either the TM mode or the TE mode, and the two reflected modes. Moreover, the incident and reflected modes propagate in different directions. Rather than deriving an explicit formula that would be complicated, $< P_{z1} >$ can be easily computed numerically in two steps. Firstly by using (2-18) and (2-19) to obtain the x and y complex components of the incident (E_i, H_i) and reflected (E_{rTM}, H_{rTM}, E_{rTE}, H_{rTE}) waves. Secondly by using these components to obtain $< P_{z1} >$ from the z component of the complex Poynting vector as

$$\langle P_{z1} \rangle = \frac{1}{2} \mathrm{Re}\, al\left[(\vec{E}_i + \vec{E}_{rTM} + \vec{E}_{rTE}) \times (\vec{H}_i^{\,*} + \vec{H}_{rTM}^{\,*} + \vec{H}_{rTE}^{\,*}) \right]_z \tag{7-17}$$

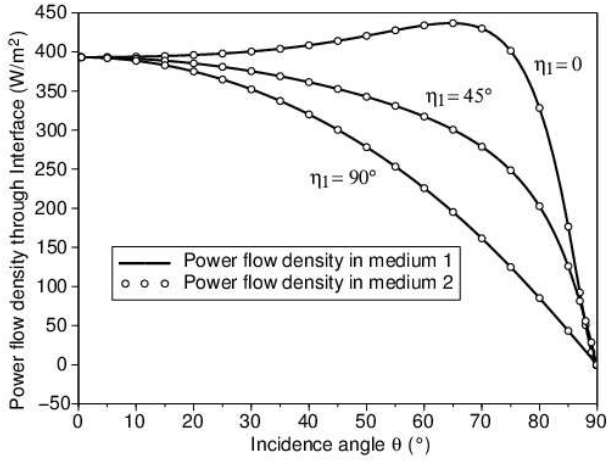

Fig. 7-3. Comparison of the average power flow density $< P_{z1} >$ in medium 1 with the average power flow density $< P_{z2} >$ in medium 2, at an interface between two media. The incident wave is the TM mode with evanescence coefficient $\cosh\chi_1 = 3$. Medium 1 is a vacuum and medium 2 is a dielectric of $\varepsilon_r = 4$.

The average power flow densities through the interface $< P_{z1} >$ and $< P_{z2} >$, computed with reflection and transmission coefficients from (7-3), are plotted in Fig. 7-3 for an interface between a vacuum and a dielectric of $\varepsilon_r = 4$. The cases $\eta_1 = 0$ and $\eta_1 = 90°$ are the special cases addressed in the above whose reflection coefficients are plotted in Figs. 7-2 and 7-1, respectively. The case $\eta_1 = 45°$ is not special, i.e. the system (7-3) that gives the reflection and transmission coefficients does not allow any simplification. As can be seen, in all the cases the conservation of energy is well verified, i.e. the power density that flows from medium 1 through the interface equals the power density that flows from the interface into medium 2.

FDTD measure of the reflection coefficient

The Huygens surface described in section IV has been also implemented with an incident wave at oblique incidence θ. In that case, the exponential in the spectra of the field components (4-1) has to take account of the evanescence in direction θ. This experimental setting has been used to compute the reflection coefficient of an evanescent wave from an interface between a vacuum and a dielectric where the speed of light is $c/3$. The method is the one used with PML interfaces in [8], with a Gaussian pulse incident wave. It consists of using a large Huygens surface in y direction, with the interface just behind its front side. However, with evanescent waves there appears a limitation in the size of the Huygens surface. Consider for instance $\cosh\chi = 1.5$, i.e. $\sinh\chi = 1.118$, and $\Delta y = 5$ cm. For frequency 250 MHz, the evanescence coefficient equals $5\ 10^{12}$ over 100 cells, and $25\ 10^{60}$ over 500 cells. This means that the field is quite inhomogeneous if the FDTD domain is large. From this, the numerical noise of the large field region propagates toward the region of interest and pollutes it. In practice, using a domain a few hundred cells in y direction, it has been possible to compute the reflection coefficient up to an incidence θ which depends on $\cosh\chi$, for instance up to θ = 15° with $\cosh\chi = 1.3$.

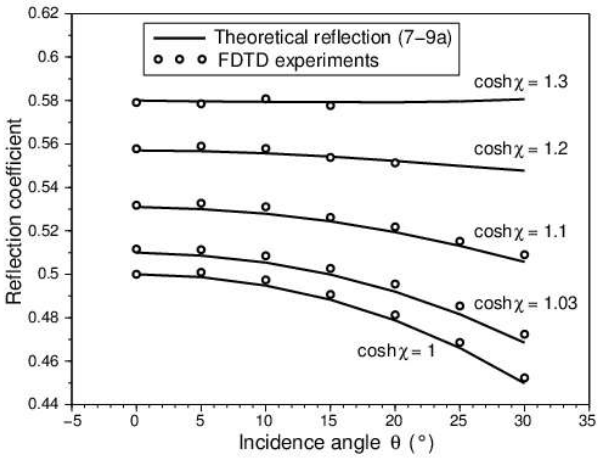

Fig. 7-4. Comparison of the theoretical reflection of the TM mode (7-9a) with the reflection computed with the 2D FDTD method, from an interface between a vacuum and a dielectric of speed $c/3$. For $\cosh\chi = 1.2$ and 1.3 some FDTD results which were strongly polluted by the noise due to the non homogeneity of the field are not represented (missing circles).

The 2D FDTD experiments have been performed with the TM mode in the case corresponding to the 3D case $\eta_1 = +\pi/2$ whose theoretical reflection is given by (7-9a). Some FDTD results are compared with the modulus of (7-9a) in Fig. 7-4 for a traveling wave ($\cosh\chi = 1$) and for four evanescent waves ($\cosh\chi$ = 1.03, 1.1, 1.2, 1.3). An excellent agreement is observed, which demonstrates the exactness of (7-9a).

VIII. Conclusion

This paper is schematically composed with two parts. The content of the first part is mainly a revisit of the evanescent plane wave solutions of the Maxwell equations in free space. They are derived and expressed differently than in the only textbook we have found on this question [5]. Especially, explicit expressions of the wavenumbers and of the field components are provided in Cartesian coordinates which renders easy the solution of some problems involving evanescent waves.

The content of the second part is probably more original, since we have not found any textbook or paper reporting similar content. Firstly the Snell law and the Fresnel coefficients of

evanescent plane waves are derived at the interface between dielectric media. Secondly, it is shown that evanescent plane waves can be enforced in the space domain of such computational methods as the FDTD method. This allows theoretical results concerning evanescent waves to be verified, as in this paper, and opens the way to numerical calculations where the source of the electromagnetic energy is composed with evanescent waves.

REFERENCES

[1] J. Stratton, "Electromagnetic Theory", IEEE Press, 2007.

[2] J. Van Bladel, "Electromagnetic Fields", IEEE Press, 2007.

[3] J. A. Kong, "Theory of Electromagnetic Waves", John Wiley & Sons, 1975.

[4] D.S. Jones, "The Theory of Electromagnetism", Pergamon Press, 1964.

[5] G.S. Smith, "An Introduction to Classical Electromagnetic Radiation", Cambridge Univ. Press, 1997.

[6] J.-P. Bérenger "Evanescent waves in PML's: Origin of the numerical reflection in wave-structure interaction problems", *IEEE Trans. Ant. Propag.*, vol. 47, pp. 1497-1503, 1999.

[7] A. Taflove, S. Hagness, "Computational electrodynamics: The finite-difference time-domain method", Artech House, 2005.

[8] J.-P. Bérenger "A perfectly matched layer for the absorption of electromagnetic waves", *J. Comp. Phys.*, vol. 114, pp. 185-200, 1994.